Int. J. Heat Mass Transfer. Vol. 27, No. 4, pp. 599–610, 1984
Printed in Great Britain

0017-9310/84 $3.00 + 0.00

THERMAL RESISTANCE AT A SURFACE IN CONTACT WITH FLUIDIZED BED PARTICLES

DAVID GLOSKI, LEON GLICKSMAN and NORMAN DECKER
Department of Mechanical Engineering, Massachusetts Institute of Technology,
Cambridge, MA 02139, U.S.A.

(*Received* 6 *September* 1982 *and in revised form* 10 *June* 1983)

Abstract—While most investigators agree that heat transfer from the dense phase of a fluidized bed is the dominant mode of heat transfer from bed to surface, models of the process have taken many disparate forms. The differences among these models are most evident with beds of large particles and at short dense phase residence times. An experimental apparatus has been developed which permits measurement of the thermal resistance between a surface and adjacent particles during a rapid transient process. Meaningful results are obtainable for periods as short as 10 ms. Large heat transfer coefficients for particles with diameters between 0.65 and 1.0 mm were observed in the initial 20 ms. During an ensuing period of about 80 ms the measured heat transfer coefficients were lower and nearly invariant with time. After that the coefficients began to decline. This behavior is most consistent with a discrete particle model with initial heat transfer by asperities in direct contact with the surface followed by heat transfer through gas layers in areas adjacent to the contact points. No significant difference was observed between minimally fluidized and packed beds of the same batch of particles, refuting the notion of a gas layer separating the particles from the surface in fluidized beds.

NOMENCLATURE

A_H	surface area of heater
C_p	specific heat capacity
c_{pH}	specific heat capacity of heater element
d_p	particle diameter
Fo	Fourier number, α_e/d_p^2
h	instantaneous heat transfer coefficient
$\bar{h}$	time averaged heat transfer coefficient
i_H	current through heater
k	thermal conductivity
k_e	thermal conductivity of emulsion
k_g	thermal conductivity of gas
Nu	instantaneous Nusselt number, hd_p/k_g
$\overline{Nu}$	time averaged Nusselt number
Nu_0	surface resistance Nusselt number
Nu_s	experimentally derived surface resistance Nusselt number
q_{bed}	rate of heat transfer from heater to bed
q_{gen}	rate of heat generation in foil
q_{st}	rate of energy storage in foil
q_{sub}	rate of heat transfer from foil to substrate
R_H	electrical resistance of heater
T_B	bed temperature
T_H	heater temperature
t	time
t_H	heater thickness
u	product, $Nu_0\, k_g/k_e \sqrt{Fo}$
U_0	gas superficial velocity
U_{mf}	superficial velocity at minimum fluidization
V_H	potential drop across heater.

Greek symbols

α_e	thermal diffusivity of emulsion
ε	mean roughness height
ρ	density
ρ_H	density of foil
τ	time constant.

INTRODUCTION

MANY fluidized beds contain immersed heat transfer surfaces to control the bed temperature and to transfer heat to or from the bed material. Numerous empirical correlations for heat transfer coefficients have been proposed based upon measurements of heat transfer between beds and surfaces immersed in them [1–5]. The correlations have been shown to give, at best, reasonable agreement with experimental data over a modest range of conditions [6, 7]. When the correlations are extrapolated using parameter values outside the range of the original data, there is the possibility of significant error.

Basic models of the heat transfer process, founded on the physical mechanisms involved, should be an improvement over purely empirical correlations. Early studies demonstrated the dominant effect of the emulsion phase in fluidized bed heat transfer. Subsequent investigations suggested that an upper bound exists, limiting the rate of heat transfer at short emulsion residence times. A clear understanding of this limit and its underlying mechanism is important, particularly in beds where the limit is approached.

In this work, heat transfer coefficients measured at very short elapsed times are compared with several models of the dense phase heat transfer transient.

MODELS FOR EMULSION HEAT TRANSFER

One of the earliest models for heat transfer from the emulsion phase to the immersed surface is due to Mickley and Fairbanks [8]. The emulsion was assumed to be a continuum with an effective conductivity and heat capacity which was uniform across the emulsion. The heat transfer was represented as a transient process from the immersed surface to the emulsion with the resulting heat flux related to the residence time of the emulsion at the surface. This model gives reasonable values for large residence times, but it leads to unrealistically high values of the heat transfer rate at low residence times. The deficiency of the homogeneous emulsion model at short times was believed to be associated with the lower density of particle packing near the heat transfer surface and the consequently greater resistance to heat transfer between the particles and the surface.

The emulsion model has been modified by Baskakov [9] and Gel'perin and Einstein [10], among others, by the introduction of a thermal resistance between the homogeneous emulsion and the heat transfer surface. The surface resistance is empirically found to be expressed as a constant times the ratio of the particle diameter to the fluid thermal conductivity. The modified emulsion model incorporating this surface resistance agrees reasonably well with experimental results. The form of the contact resistance indicates that it can be considered as a conduction resistance through the fluid with a characteristic conduction distance related to the particle diameter. However, a more exact understanding of the phenomena near the heat transfer surface is lacking.

Botterill [11] presented an alternate representation of the region near the surface. He considered the transient heat transfer between one or two rows of individual spherical particles at a planar heat transfer surface. It can be shown that for short residence times, or for larger particles at longer residence times, e.g. 0.3 s for 1 mm particles, that the temperature change of the emulsion is confined to a region only one or two particle layers from the surface [12]. Thus, the use of individual particles to model the contact region is a closer physical representation of the actual process than the use of a homogeneous continuum model. However, when the particles were assumed to touch the surface, Botterill's numerical results overpredicted the total heat flux. It is important to note that Botterill assumed that the particles were perfect spheres and the heat transfer surface a perfect plane. When the particle contacts the surface, the region near the contact point is microscopic in size. The use of perfect geometry for the sphere and plane results in a very small clearance between particles and the surface near the contact region and consequently a very high integrated heat flux. Because of the high flux calculated when the particle was assumed to contact the surface it was concluded that the particles did not touch the surface; rather, a thin fluid film was interposed to separate the particles and the surface. The film thickness was empirically chosen to give the best agreement with experimental results.

Although other authors have doubted the presence of a thin film between the particles and the adjacent surface, it has been included as necessary to achieve reasonable results [13]. If the thermal resistance is due to a gas layer between the surface and the first row of particles, the maximum heat transfer rate at short residence times will not exceed the steady state conduction across the gas layer with the particles at the bed temperature. This is due to the low heat capacity of the gas layer; the initial transient heating of the gas layer will take a fraction of a millisecond for a gas layer 0.1 mm thick. Thinner layers will take even shorter times to achieve steady state.

A different approach is taken by Kubie and Broughton [14] and Chandran [15]. The continuum concept of the emulsion is retained right up to the heat transfer surface, but the effective thermal conductivity and the heat capacity of the emulsion are taken as variable within one particle diameter of the surface. Within the range of data available, the continuum model with variable properties gives results comparable with the results from models composed of a uniform continuum with a surface resistance. However, the application of any continuum model to a layer one to two particle diameters thick when there is a large discontinuity between particle and fluid properties is open to question. The variable property model predicts much higher heat fluxes than the surface resistance model for very short residence times, of the order of 50 ms and less. This characteristic will prove useful to evaluate the accuracy of the variable property model.

The uncertainty in predicting the emulsion heat transfer lies in an inadequate representation of the contact resistance. For small particles, the influence of the contact resistance on the overall heat transfer increases as the residence time of the emulsion decreases. The heat transfer experiments performed in freely bubbling beds which will include a range of emulsion contact times tends to obscure the influence of the contact resistance.

It has been shown that for large particles the total thermal resistance is concentrated in the region between the surface and the first row of particles [12]. Thus, a more thorough understanding of the heat transfer close to the surface is important for large particles.

CONTACT RESISTANCE NEAR THE HEAT TRANSFER SURFACE

Schlünder [16] retained the assumption of perfect spherical particles in contact with a perfect planar wall. He accounted for the thermal resistance by allowing for a diminished heat transfer rate in the gas in regions where the distance between the particle and surface is less than the mean free path of the fluidizing gas. Reasonable results were obtained for the contact resistance; however, the thermal accommodation coefficient used by Schlünder is an order of magnitude less than the usually accepted values. The model of Schlünder does not account for heat transfer through areas of direct particle-to-surface contact; all contact regions are assumed to be point contacts. Because of the assumption of ideal geometry, this model is only appropriate when the height of the surface roughness of the particle and heat transfer surface is less than the mean free path of the gas molecules.

Decker and Glicksman [17] modeled the particle and heat transfer surface as real surfaces which have

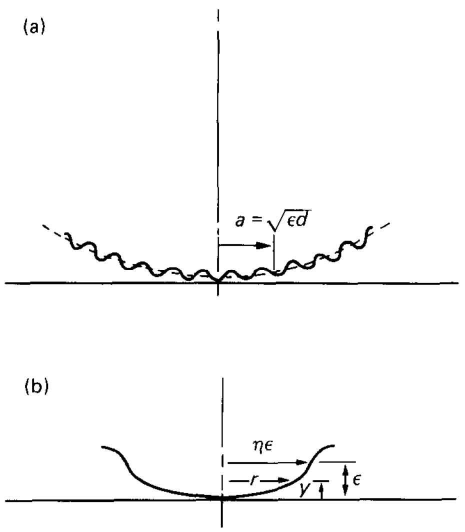

FIG. 1. (a) Contact zone geometry, (b) asperity geometry.

solid-to-solid contact at a limited number of microscopic roughness elements. Due to the small size and limited heat capacity of the roughness asperities, very high heat transfer rates occur for only the first 10–20 ms of the contact time. During this time the contact zone of the asperities approaches a mean temperature between that of the surface and the bed. This is followed by a longer period of more slowly declining rate of heat transfer until the average temperature of the entire particle changes appreciably. The initial period of high heat transfer rate occurs so rapidly that its influence on the time averaged heat transfer is negligible for typical contact times observed in fluidized beds.

Figure 1 shows the contact geometry assumed by Decker and Glicksman. Figure 2 shows typical results for the surface Nusselt number after the initial short time transient has died away. The Nusselt number is defined based on the average heat flux, the surface temperature, and the bulk bed temperature. Note that the surface Nusselt number remains practically constant over a wide range of roughness. Furthermore, it is quite insensitive to the properties of the particle and the heat transfer surface. These characteristics are consistent with previous experimentally determined surface resistance values which indicate that the surface resistance is relatively unaffected by these variables. The surface Nusselt numbers displayed in Fig. 2 are based upon the heat transfer through the particle projected area, $\pi d^2/4$, only. In application they are multiplied by the area fraction of particles projected on the surface, roughly 0.5.

Figure 3 compares four models of the emulsion heat transfer. In each model the boundary condition at the wall is a step increase in temperature from the bed temperature to a constant wall temperature. The Mickley and Fairbanks homogeneous continuum model provides an upper bound as well as an asymptote approached by the other continuum models at large residence times (large Fourier numbers)

$$\overline{Nu} = \frac{2}{\sqrt{(\pi\, Fo)}}\frac{k_e}{k_g}. \tag{1}$$

Chandran [15] solved the variable property continuum model numerically to yield the curve shown. Results were shown only for Fourier numbers greater than 10^{-3}. The asymptote that this model approaches at small Fourier numbers was found using a similar-

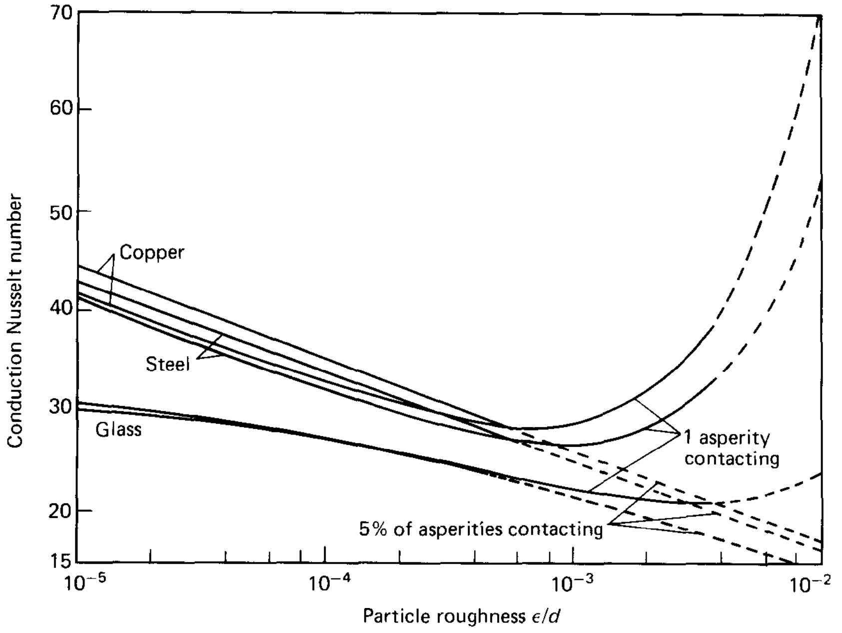

FIG. 2. Predicted surface conduction Nusselt numbers for various materials.

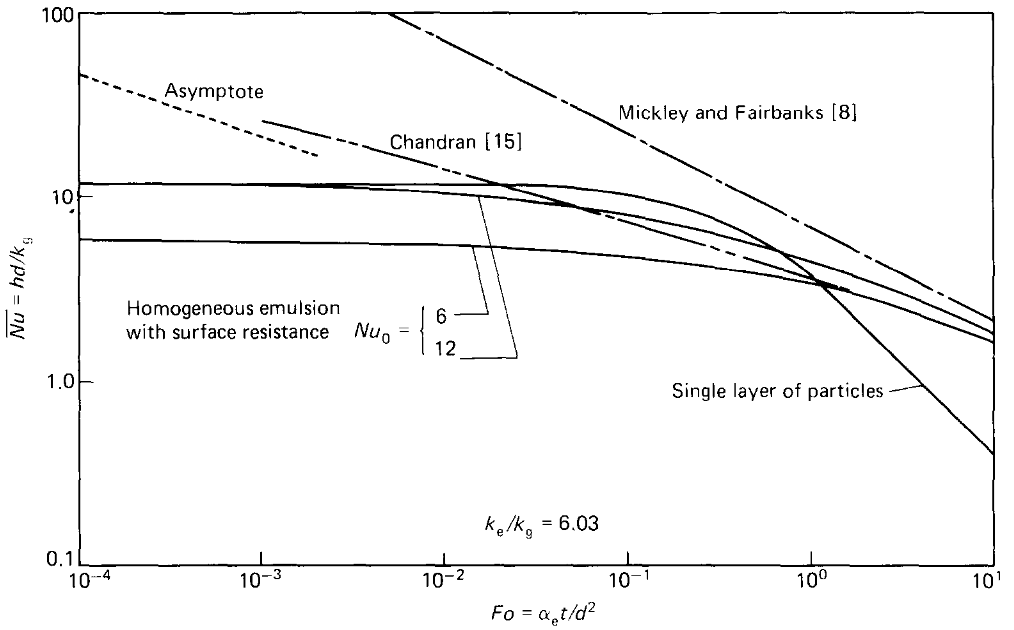

FIG. 3. A comparison of various models of the time-averaged Nusselt number.

ity solution, included here as an appendix, of the differential equation obtained by allowing the density, but not the thermal conductivity, of the continuum to increase with distance from the wall. It consequently yields a lower bound to the numerical solution of Chandran's equation

$$\overline{Nu} = \frac{3^{2/3}}{2\Gamma(4/3)}\left(\frac{k_e}{k_g}\right)^{1/3}(Fo)^{-1/3}, \qquad (2)$$

where $\Gamma(4/3)$ is the gamma function of 4/3 and equals 0.893.

Modeling the emulsion as a single layer of particles with uniform but time-varying temperature and in thermal communication with the wall only yields

$$\overline{Nu} = \frac{2k_e}{3K_g Fo}\left[1-\exp\left(-\frac{3}{2}Nu_0\frac{k_g}{k_e}Fo\right)\right], \qquad (3)$$

where Nu_0 is the Nusselt number associated with the surface resistance, here taken as 12. This is included predominantly to illustrate the range of Fourier numbers over which the effects of the first layer of particles are dominant.

Modeling the emulsion as a homogeneous continuum with a surface resistance [10] provides

$$\overline{Nu} = \frac{Nu_0}{u^2}\left[e^{u^2}\operatorname{erfc} u - 1 + \frac{2u}{\sqrt{\pi}}\right], \qquad (4)$$

where

$$u = Nu_0\frac{k_g}{k_e}\sqrt{Fo}.$$

This function, like the previous one, is completely dominated by Nu_0 at low Fourier numbers. This model is shown for two values of Nu_0; 12 and 6. For Fourier numbers greater than unity, both of these curves closely follow Chandran's numerical solution.

PREVIOUS EXPERIMENTAL RESULTS

Clearly, results from well-controlled experiments are needed to carry out a critical evaluation of the proposed models for surface resistance. Figure 4, taken from Kubie and Broughton [14] shows a typical comparison of existing data with their variable property emulsion model. Kubie and Broughton imposed a constant heat flux boundary condition at the wall in their numerical solution shown. Superimposed on Fig. 4 is the homogeneous emulsion model with a constant surface resistance and with a constant temperature boundary condition assumed at the wall. In the range of Fourier numbers for the data, both models are equally valid. At these Fourier numbers, the thermal gradient has moved sufficiently deep into the emulsion phase tending to obscure the influence of the phenomena directly adjacent to the heat transfer surface. Thus, data is needed at lower Fourier numbers to more closely evaluate the surface contact model. Dunsky *et al.* [18] have carried out experiments with a small heated object rotated through a fluidized bed to provide time averaged Nusselt numbers at lower Fourier numbers. The influence of the moving object on the surface alignment of particles is difficult to define and the surface conditions are neither constant heat flux nor constant surface temperature. Thus, it is difficult to draw an exact parallel between these results and those in a conventional fluidized bed. They correlated their maximum heat transfer coefficients from their time average data with a dimensional expression. Relating these maximum coefficients as representative of surface

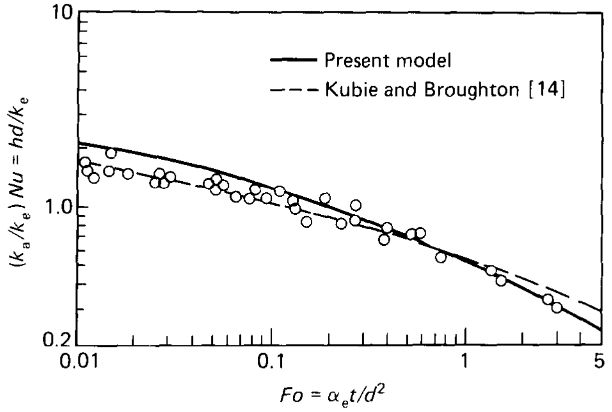

FIG. 4. A comparison of the present model with that of Kubie and Broughton [14] and data of Antonishin cited by Kubie and Broughton for moderate to large Fourier numbers.

resistances, their expression would be

$$Nu_0 = 6.6 + Cd_p/k_g, \tag{5}$$

where C is a dimensional constant equal to 57 W m^{-2} °C^{-1} or 10 Btu h^{-1} ft^2 °F^{-1}. Baskakov *et al.* [19] demonstrated a reasonable fit of data to a model with a surface resistance. Their surface resistance, expressed as a Nusselt number, would be

$$Nu_0 = 2k_e/k_g. \tag{6}$$

This same expression represents the surface resistance suggested by Gel'perin and Einstein [10]. The surface resistance was also evaluated by Catipovic *et al.* [20], but by subtracting the heat transfer coefficient at minimum fluidizing velocity from the measured maximum instantaneous heat transfer coefficient. Their results suggested a value of 6.0 for Nu_0.

The purpose of the present experiments is to provide data at low Fourier number for well-defined configurations. A transient technique has been developed which allows the contact resistance to be measured for both packed and fluidized beds over a variety of particle sizes and gas velocities.

EXPERIMENTAL APPARATUS AND DATA REDUCTION

The experimental apparatus was designed to obtain measurements of the emulsion heat transfer coefficient at low Fourier numbers. Instead of initiating the transient by the transport of particles to or across a preheated surface, the process takes place with a stationary bed and heater. The heater is then rapidly heated to initiate the transient. This method allows for the acquisition of data, within the contact resistance region, for packed and incipiently fluidized beds.

Figure 5 shows the heater module which, when mounted into the wall of the bed, allows a thin tin foil heater to form a portion of the inner wall of the bed. The thermal transient is initiated by discharging a capacitor through the heater circuit. Following this initial power surge, which rapidly increases the foil temperature, the power supply maintains the foil temperature approximately constant with time. The rate of heat generation within the heater, $q_{\text{gen}}(t)$, is given by

$$q_{\text{gen}}(t) = V_{\text{H}}(t)i_{\text{H}}(t), \tag{7}$$

where $i_{\text{H}}(t)$ and $V_{\text{H}}(t)$ are the measured values for current

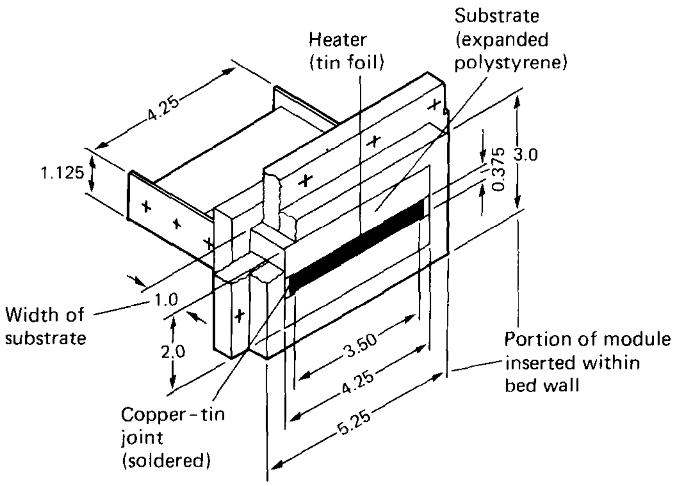

FIG. 5. Heater module: front view (all dimensions in inches).

through and potential drop across the heater, respectively. Heater temperature was carefully correlated with the heater's electrical resistance

$$T_H(t) = f(R_H(t)), \tag{8}$$

which can be monitored during the transient as

$$R_H(t) = \frac{V_H(t)}{i_H(t)}. \tag{9}$$

The rate of change of energy stored within the heater is given by

$$q_{st}(t) = \rho_H A_H t_H c_{pH} \frac{dT_H(t)}{dt}. \tag{10}$$

The substrate material upon which the heating element is mounted, is treated as a homogeneous semi-infinite medium undergoing a temperature transient at its surface. The assumption of substrate behavior as a semi-infinite medium is justified by comparing the thermal penetration distance of only 0.16 in. (in a transient of 1.0 s duration) with the substrate thickness of 1.0 in. Through use of Duhamel's Theorem [21] the rate of heat transfer from the heater into the substrate is

$$q_{sub}(t) = \frac{1}{\sqrt{\pi}} [k\rho c_p]_{sub} A_H \int_0^t \frac{1}{t-s} \frac{dT_H(s)}{ds} \, ds. \tag{11}$$

The rate of heat transfer to the bed material is obtained by

$$q_{bed}(t) = q_{gen}(t) - q_{st}(t) - q_{sub}(t). \tag{12}$$

Figure 6 suggests the physical nature of these quantities.

The time-resolved emulsion heat transfer coefficient is given by

$$h(t) = \frac{q_{bed}(t)}{A_H(T_H(t) - T_B)}, \tag{13}$$

and using the surface area mean particle diameter, d_p, and the gas thermal conductivity, k_g, this is non-dimensionalized to form an emulsion Nusselt number

$$Nu(t) = \frac{h(t)d_p}{k_g}. \tag{14}$$

This emulsion Nusselt number can be modified to form a surface Nusselt number by correcting for the changing mean temperature of the particle. This modification is accomplished by the expression (detailed by Gloski [22])

$$Nu_s(t) = Nu(t)\, e^{t/\tau}, \tag{15}$$

where

$$\tau = \frac{2(\rho c_p)_p d_p}{3\bar{h}}, \tag{16}$$

and $\bar{h}$ is the single particle heat transfer coefficient determined from an analysis detailed elsewhere using the values of Nu [22].

The tin foil heater and the expanded polystyrene substrate were selected so as to maximize the sensitivity of the temperature measurement by means of the large temperature coefficient of resistivity of the tin and to minimize the rates of energy storage in the heater and substrate. Even with this choice of materials, the heat transfer to the substrate is a substantial fraction of the overall heater output for elasped times between 10 and 100 ms, being between one quarter of and equal to the heat transfer to the bed. Consequently, the heater/substrate module was calibrated in transient tests in still air to yield an effective value for the $[k\rho c_p]_{sub}$ product in equation (11).

Note that tests reported by previous authors used substrates with much higher densities and thermal conductivities, making it much more difficult to resolve the net heat transfer to the bed at short times. With a glass substrate, for example, the heat transferred to the substrate in 100 ms is ten times that transferred to the bed.

Details of the structural design and the electrical circuitry required for the experiments can be found in ref. [22]. A Hewlett-Packard Structural Dynamics

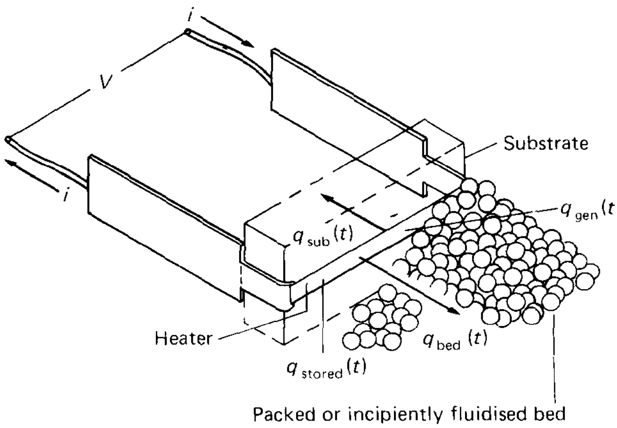

FIG. 6. Energy transfers indicating the general theory of the experiment.

Table 1

Mean particle size (U_{mf})	Particle sizes within distribution (mm)	Average weight fraction from sampling
1 mm (67.5 cm s^{-1})	1	1.00
0.744 mm (41.0 cm s^{-1})	0.64	8.95×10^{-3}
	0.66	1.01×10^{-2}
	0.69	4.88×10^{-2}
	0.71	2.18×10^{-1}
	0.74	2.94×10^{-1}
	0.76	2.11×10^{-1}
	0.79	1.08×10^{-1}
	0.81	8.11×10^{-2}
	0.84	2.07×10^{-2}
0.645 mm (34.5 cm s^{-1})	0.48	2.10×10^{-3}
	0.51	2.41×10^{-3}
	0.53	5.66×10^{-3}
	0.56	3.20×10^{-3}
	0.58	5.82×10^{-2}
	0.61	1.77×10^{-1}
	0.64	2.49×10^{-1}
	0.66	2.68×10^{-1}
	0.69	1.81×10^{-1}
	0.71	4.37×10^{-2}
	0.81	1.00×10^{-2}

Analyzer was used for data acquisition and processing. The analyzer has two 12-bit A/D convertors which allowed simultaneous current and potential drop measurements. Due to complexity in the data reduction process, Nusselt numbers are reported only for discrete times: 10, 20, 40, 60, 80, 100, 120, and 140 ms. An error analysis indicates that the uncertainty in the resultant Nusselt numbers is ±8%.

RESULTS

Experiments were carried out with three different sizes of glass spheres: uniform size 1 mm spheres, and narrow cut mixtures of particles with mean diameters of 0.74 and 0.65 mm, respectively. Table 1 presents the size distribution for each mixture and the measured minimum fluidization velocity.

Figure 7 shows the temperature of the heater foil over the duration of one test. The foil temperature reaches the desired temperature level within 10 ms and remains approximately at that level over the course of the experiment; the accuracy of the data reduction is not dependent on achieving an exactly constant heater temperature.

Figures 8 and 9 show the instantaneous surface heat transfer coefficient as a function of time, non-dimensionalized as a Nusselt number based on the particle diameter and the gas conductivity. Test results are shown for gas flow conditions slightly above and below the minimum fluidizing velocity. There is a rapid decrease in the Nusselt number during the first 10–20 ms. At longer times, the instantaneous Nusselt number remains constant within the level of experimental uncertainty. The results for the packed bed are almost identical with those for the minimally fluidized bed. Thus, the surface packing is very similar for both cases. The elevated Nusselt numbers at short times are due to conduction heat transfer between the surface asperities on the particle which are in contact with the heat transfer surface. These elevated Nusselt numbers could not persist for 10 or 20 ms if a gas film separated the particles from the surface; transient effects due to heating of this gas layer would disappear in less than 1 ms.

After the surface asperities have reached a mean temperature between the bulk bed and the surface, a constant heat transfer coefficient between the particle and the surface prevails. Note that these results for the surface Nusselt number have been corrected to account for changes in the mean particle temperature with time. Thus the Nusselt number represents the thermal

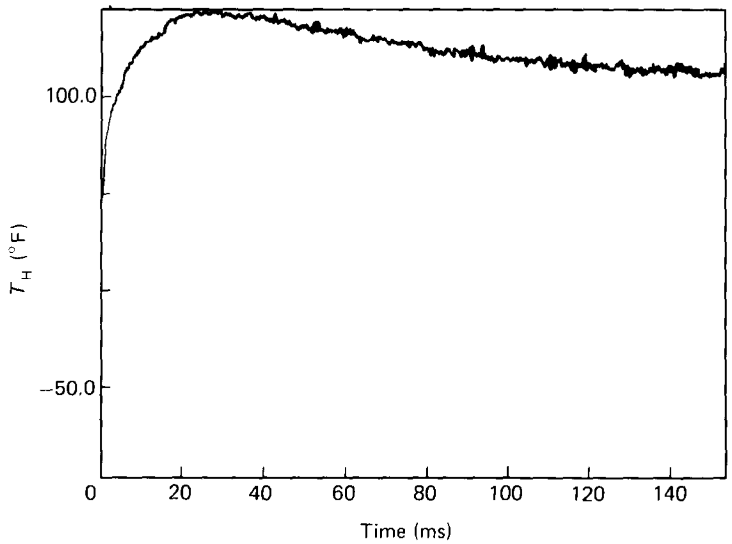

FIG. 7. Typical resulting plot of T_H vs time.

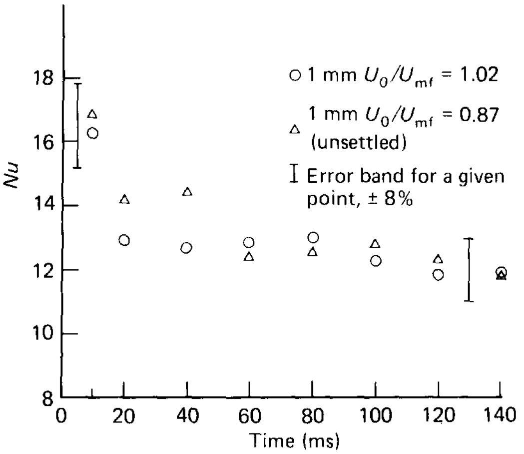

FIG. 8. Results slightly above and below U_{mf} for a mean particle diameter of 1.0.

resistance between the surface and the first row of particles. The constant value of the Nusselt number is due to the resistance primarily due to conduction through the gas layer between the particles and the surface. The close similarity between the results above and below U_{mf} indicates that a model of the emulsion as a fixed bed, unsettled by vibration or other effects, is valid up to the heat transfer surface. Furthermore, the particles in the fluidized bed are in contact with the heat transfer surface, in contradiction to the concept of a gas layer separating the particles from the surface.

When the packed bed is vibrated to settle the particles before testing there is a noticeable difference in the initial heat transfer values for 1 mm particles as seen in Fig. 10. This is due to the increase in the number of particles in contact with the heat transfer surface. At longer times when the heat transfer through the contact points is negligible, the effects of settling are not distinguishable.

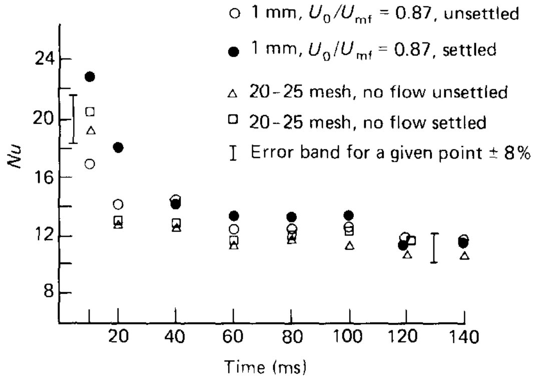

FIG. 10. Settled vs unsettled.

Figure 11 shows the effect of gas velocity on the surface resistance for the largest particles, 1 mm. Since the bed had to be restrained at higher gas velocity to prevent severe bubbling which could damage the foil heater, the bed approaches fixed bed packing. Although there should be a gas convective augmentation of the surface resistance as the velocity increases, the increase predicted by Glicksman and Decker [23] is only about 1.6 for the maximum flow rate displayed in Fig. 11, being proportionally smaller for the smaller flow rates. Within the experimental uncertainty of the data this effect is not readily apparent. Note also that this experimental configuration, with a very short heater length in the direction of the gas flow, is not identical to a real heat exchanger surface where a longer heated length is traversed by the airflow.

COMPARISON WITH OVERALL MODELS

Data for the three particle sizes at low Fourier numbers are compared in Fig. 12 with the instantaneous Nusselt numbers predicted by the homogeneous emulsion/surface resistance model

$$Nu = Nu_0\, e^{u^2} \operatorname{erfc} u. \tag{17}$$

In each case a value of 12 has been assumed for Nu_0. Shown also is the lower bound asymptotic solution to the variable property continuum model of Chandran

$$Nu = \left(\frac{1}{3}\right)^{1/3} \frac{1}{\Gamma(4/3)} \left(\frac{k_e}{k_g}\right)^{1/3} Fo^{-1/3}. \tag{16}$$

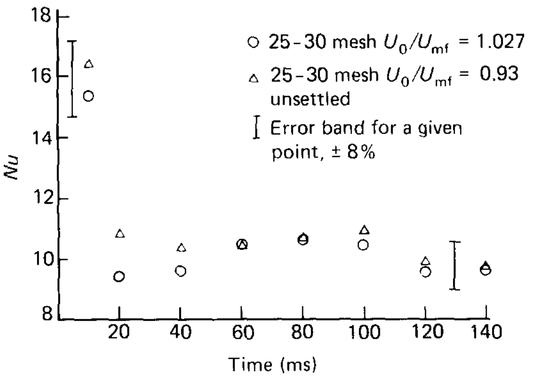

FIG. 9. Results slightly above and below U_{mf} for a mean particle diameter of 0.645.

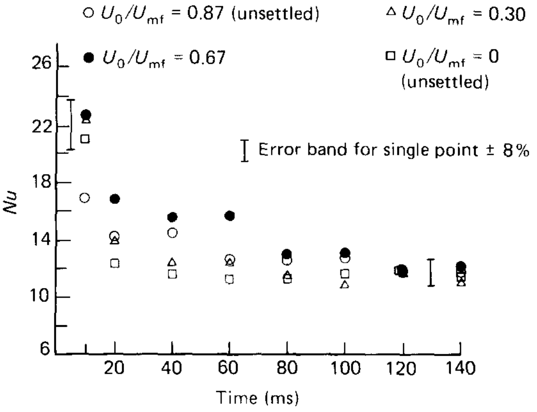

FIG. 11. Velocity effects for 1 mm particles.

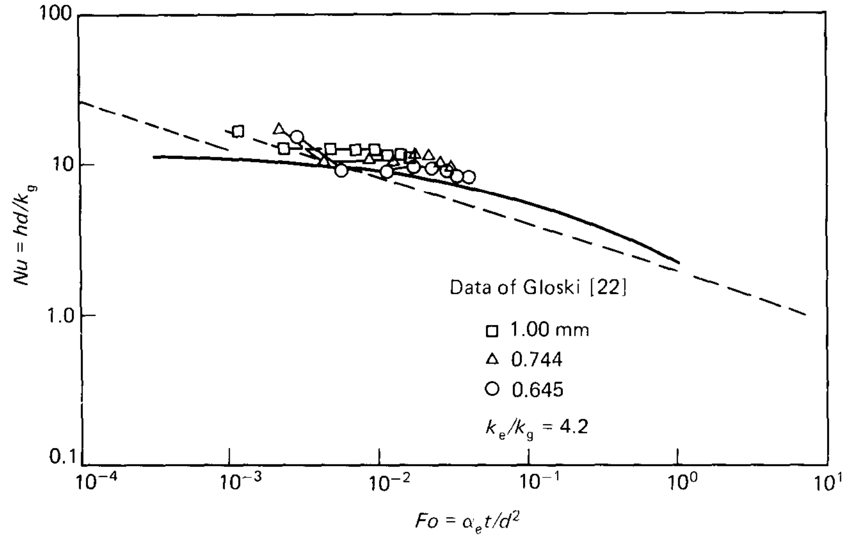

FIG. 12. Instantaneous Nusselt number, a comparison of the data of Gloski with the present model. Shown also (dashed line) is the Chandran model and its asymptote.

Figure 13 displays a similar comparison of the data of Dunsky *et al.* for time-averaged emulsion heat transfer with the corresponding homogeneous emulsion/surface resistance model and the asymptotic lower bound of the variable property continuum model.

Almost all of the remaining data in the literature is for higher Fourier numbers. It is clear from Fig. 13 that at high Fourier numbers it is impossible to properly evaluate the relative accuracy of the various models, since they all yield similar results. Even when the value of the surface resistance is varied for the homogeneous emulsion plus surface resistance model, the differences are minimal at higher *Fo* values.

Results at lower *Fo* levels where the surface effects are pronounced provide a clearer indication of the validity of the proposed model. Note that the variable property emulsion model when extended to low values of *Fo* deviates significantly from the measured behavior.

For short contact times a model using a single row of particles at uniform temperature separated from the surface by a thermal contact seems appropriate.

For short to intermediate contact times it is important to know the thermal contact resistance. At present, there is not enough data to determine how the contact resistance varies with particle sphericity, size distribution or thermal physical properties.

For typical bed operating conditions where relatively long contact times occur, the constant emulsion model with a surface resistance gives adequate accuracy given the present uncertainty in key parameters. It also has the advantage of a relatively simple closed form solution.

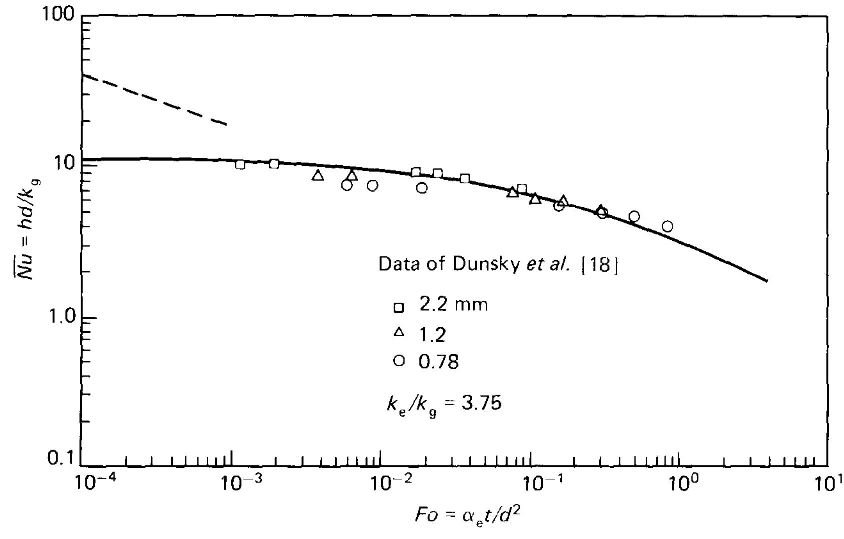

FIG. 13. Time-averaged Nusselt number, a comparison of the data of Dunsky *et al.* with the present model. Shown also (dashed line) is the asymptote of the Chandran model.

CONCLUSION

An experimental technique has been developed which permits the heat transfer between the surface and particles to be measured for both fixed and fluidized beds.

Results for fixed and fluidized beds at vertical heat transfer surfaces were virtually identical. In both cases at times of 20 ms or less, very high Nusselt numbers were observed which are due to direct heat transfer between particle and surface asperities which are in contact. At longer times a constant surface Nusselt number was observed. The absence of any significant difference between the packed bed and fluidized bed results suggests that there need not be an intervening gas layer between the contact points on the surface and the particles of a fluidized bed.

The constant Nusselt number found after the initial transient suggests that the heat transfer from the surface to the particle takes place primarily through the fluid separating the particle and the surface. The greater local resistance at the surface, after the initial 20 ms, must be due to the greater local voidage there. One-dimensional models reflecting this voidage distribution may be inadequate since they neglect the inhomogeneous distribution of thermal properties. Their numerical complexities may not be warranted in light of this uncertainty.

Further work needs to be done to determine the influence of particle sphericity and the distribution of particle sizes.

Acknowledgements—The work was supported in part by the National Science Foundation. David Gloski would like to acknowledge the support of the American Electric Power Corporation.

REFERENCES

1. H. A. Vreedenberg, Heat transfer between a fluidized bed and a horizontal tube, *Chem. Engng Sci.* **9**, 52–60 (1958).
2. B. R. Andeen and L. R. Glicksman, Heat transfer to horizontal tubes in shallow fluidized beds, ASME paper 76-HT-67 (1976).
3. F. W. Staub, Solid circulation in turbulent fluidized beds and heat transfer to immersed tube banks, *J. Heat Transfer* **101**, 391–396 (1979).
4. J. S. M. Botterill and A. O. O. Denloye, Gas convective heat transfer to packed and fluidized beds, *A.I.Ch.E. Symp. Ser.* **74** (176), 194–202 (1978).
5. N. S. Grewal and S. C. Saxena, Experimental studies of heat transfer between bundle of horizontal tubes and a gas–solid fluidized bed, ASME paper 80-HT-119 (1980).
6. J. S. M. Botterill, Y. Teoman and K. R. Yuregir, Temperature effects on the heat transfer behaviour of gas fluidized beds, *A.I.Ch.E. Symp. Ser.* **77** (208), 330–340 (1981).
7. P. J. Shah, S. N. Upadhyay and S. C. Saxena, Heat transfer from large diameter smooth horizontal tubes immersed in gas fluidized beds, presented at 20th National Heat Transfer Conf., Session 30, Milwaukee, Wisconsin, 2–5 August (1981).
8. H. S. Mickley and D. F. Fairbanks, Mechanism of heat transfer to fluidized beds, *A.I.Ch.E. Jl*, **1**, 374–384 (1955).
9. A. P. Baskakov, The mechanism of heat transfer between a fluidized bed and a surface, *Int. Chem. Engng* **4**, 320–324 (1964).
10. N. I. Gel'perin and V. G. Einstein, Heat transfer in fluidized beds, in *Fluidization* (edited by J. F. Davidson and D. Harrison). Academic Press, London (1971).
11. J. S. M. Botterill, *Fluid-bed Heat Transfer*. Academic Press, London (1975).
12. L. R. Glicksman and N. Decker, Heat transfer from an immersed surface to adjacent particles in a fluidized bed: the role of radiation and particle packing, *Proc. 7th Int. Heat Transfer Conf.*, Munich, September (1982).
13. J. D. Gabor, Wall-to-bed heat transfer in fluidized and packed beds, *Chem. Engng Prog. Symp. Ser.* **66** (105), 76–86 (1970).
14. J. Kubie and J. Broughton, A model of heat transfer in gas fluidized beds, *Int. J. Heat Mass Transfer* **18**, 289–299 (1975).
15. R. Chandran, Local heat transfer and fluidization dynamics around horizontal tubes in fluidized beds, Ph.D. dissertation, Lehigh University, Bethlehem, Pennsylvania (1980).
16. E. U. Schlünder, Warmeubergang an bewegte kugelschutengen bei kurzfristigem kontakt, *Chemie–Ingr–Tech.* **43**, 651–654 (1971).
17. N. A. Decker and L. R. Glicksman, Conduction heat transfer at the surface of bodies immersed in gas fluidized beds of spherical particles, *A.I.Ch.E. Symp. Ser.* **77** (208), 341–349 (1981).
18. V. D. Dunsky, S. S. Zabrodsky and A. I. Tamarin, On the mechanism of heat transfer between a surface and a bed of moving particles, *Proc. 3rd Int. Heat Transfer Conf.*, Vol. 4, pp. 293–297. A.I.Ch.E. (1966).
19. A. P. Baskakov, B. V. Berg, O. K. Vitt, N. F. Filippovsky, V. A. Kiradosyan, J. M. Goldobin and V. K. Maskaev, Heat transfer to objects immersed in fluidized beds, *Power Technol.* **8**, 273–282 (1973).
20. N. M. Catipovic, G. N. Jovanovic, T. J. Fitzgerald and O. Levenspiel, A model for heat transfer to horizontal tubes immersed in a fluidized bed of large particles, in *Fluidization* (edited by J. R. Grace and J. M. Matsen). Plenum Press, New York (1980).
21. V. S. Arpaci, *Conduction Heat Transfer*. Addison-Wesley, Reading, Massachusetts (1966).
22. D. Gloski, An experimental study of the transient particle–wall thermal contact resistance in fluidized and packed beds, M.S. thesis, Department of Mechanical Engineering, MIT, Cambridge, Massachusetts (1981).
23. L. R. Glicksman and N. A. Decker, Design relationships for predicting heat transfer to tube bundles in fluidized bed combustors, *Proc. 6th Int. Conf. on Fluidized Bed Combustion*, Atlanta, Georgia, U.S. Dept. of Energy, CONF-800428 (1980).

APPENDIX

SOLUTION OF THE VARIABLE PROPERTY CONTINUUM MODEL AT SMALL TIME

In the models of Kubie and Broughton [14] and of Chandran [15] the effective thermal conductivity and heat capacity of the emulsion are taken as variable within one particle diameter of the surface. Solution of the resulting differential equation generally requires a numerical solution to determine the Nusselt number as a function of the Fourier number. Solution at very small Fourier numbers is not given due to the need for very small increments in the spatial and temporal variables.

A closed form solution for Chandran's model can be achieved in the limit of small Fourier numbers. The heat transfer in that instance is confined to a layer whose thickness is small compared with a particle diameter. For small x/d_p the property variations assumed by Chandran and Kubie, and

Broughton can be approximated as

$$\rho c \sim 3x/d_{\mathrm{p}}\,(\rho c)_{\mathrm{e}}, \tag{A1}$$

and

$$k \sim k_{\mathrm{g}}. \tag{A2}$$

The differential equation for the emulsion phase becomes

$$3x/d_{\mathrm{p}}\,(\rho c)_{\mathrm{e}}\frac{\partial T}{\partial t} = K_{\mathrm{g}}\frac{\partial^2 T}{\partial x^2}. \tag{A3}$$

Chandran's boundary conditions (constant wall temperature solution) are

$$T(0,x) = T_0,$$

$$T(t > 0,0) = T_{\mathrm{w}},$$

$$\frac{\partial T}{\partial x}(t, x \to \infty) \to 0.$$

Applying the similarity transformation $\eta = x/t^{1/3}$ the partial differential equation becomes an ordinary differential equation

$$-\eta^2\frac{\mathrm{d}T}{\mathrm{d}y} = \frac{k_{\mathrm{g}}d_{\mathrm{p}}}{(\rho c)_{\mathrm{e}}}\frac{\mathrm{d}^2T}{\mathrm{d}y^2}. \tag{A4}$$

This can be integrated to find the temperature gradient

$$\frac{\mathrm{d}T}{\mathrm{d}y} = C_0\,\mathrm{e}^{-(\eta^3(\rho c)_{\mathrm{e}}/3k_{\mathrm{g}}d_{\mathrm{p}})}. \tag{A5}$$

From this, the instantaneous Nusselt number can be found to be

$$Nu = \left(\frac{1}{3}\right)^{1/3}\frac{1}{\Gamma(4/3)}\left(\frac{k_{\mathrm{e}}}{k_{\mathrm{g}}}\right)^{1/3} Fo^{-1/3}, \tag{A6}$$

and the time-averaged Nusselt number is

$$\overline{Nu} = \frac{3^{2/3}}{2\Gamma(4/3)}\left(\frac{k_{\mathrm{e}}}{k_{\mathrm{g}}}\right)^{1/3} Fo^{-1/3}. \tag{A7}$$

The constant heat flux problem solved numerically by Kubie and Broughton does not lend itself to this similarity solution method.

RESISTANCE THERMIQUE DE CONTACT ENTRE UNE SURFACE ET LES PARTICULES D'UN LIT FLUIDISE

Résumé—Alors que la plupart des chercheurs pensent que le transfert thermique de la phase dense d'un lit fluidisé est le mode dominant dans le transfert du lit à la surface, les modèles du mécanisme prennent des formes très disparates. Les différences entre ces modèles sont plus évidents pour les lits à grosses particules et à courts temps de résidence dans la phase dense. Un montage expérimental permet la mesure de la résistance thermique entre une surface et les particules adjacentes pendant un processus bref. Des résultats sont obtenus pour des séquences aussi courtes que 10 ms. Des grands coefficients de transfert pour des particules ayant des diamètres entre 0,65 et 1,0 mm sont observés pendant 20 ms initiales. Pendant une période suivante de 80 ms environ, les coefficients de transfert sont plus faibles et presque indépendants du temps. Ensuite les coefficients commencent à décroître. Ce comportement est plus compatible avec un modèle discret de particules avec un transfert thermique initial par des aspérités en contact direct avec la surface, suivi d'un transfert thermique à travers des couches de gaz adjacentes aux points de contact. On n'observe pas de différence significative entre les lits fixes ou faiblement fluidisés de particules du même réservoir, ce qui réfute la notion d'une couche gazeuse séparant les particules de la surface, dans les lits fluidisés.

DER THERMISCHE WIDERSTAND AN EINER OBERFLÄCHE, DIE MIT PARTIKELN EINES FLIESSBETTS IN BERÜHRUNG IST

Zusammenfassung—Während die meisten Forscher der Ansicht sind, daß der Wärmeübergang von der dichten Phase eines Fließbetts den überwiegenden Teil des Wärmeübergangs des Betts zur Oberfläche ausmacht, haben Modelle des Vorgangs sehr unterschiedliche Formen. Die Unterschiede dieser Modelle werden am besten sichtbar, wenn das Bett große Partikel enthält und wenn die Verweilzeiten der dichten Phase kurz sind. Dazu wurde eine Versuchsanordnung entwickelt, die die Messungen des thermischen Widerstands zwischen Oberfläche und den anliegenden Partikeln während eines schnell verlaufenden Übergangsprozesses gestattet. Man bekommt aufschlußreiche Ergebnisse für Zeitabschnitte bis zu 10 ms. Es wurden große Wärmeübergangskoeffizienten für Partikeldurchmesser zwischen 0,65 und 1,0 mm während der ersten 20 ms beobachtet. Während der nachfolgenden Zeitspanne von 80 ms waren die gemessenen Wärmeübergangskoeffizienten kleiner und nahezu unabhängig von der Zeit. Danach wurden die Koeffizienten wider kleiner. Dieses Verhalten läßt sich gut mit einem diskreten Partikelmodell erklären, wobei der Wärmeübergang nur an Rauhigkeiten mit direktem Kontakt zur Oberfläche stattfindet, gefolgt vom Wärmeübergang durch Gasschichten in den an die Kontaktstelle angrenzenden Gebieten. Es wurden keine wesentlichen Unterschiede zwischen leicht gelockerten Fließbetten und Festbetten mit den gleichen Partikeln festgestellt. Die Vorstellung einer trennenden Gasschicht zwischen den Partikeln und der Oberfläche in Fließbetten wird damit widerlegt.

ТЕПЛОВОЕ СОПРОТИВЛЕНИЕ НА ПОВЕРХНОСТИ, КОНТАКТИРУЮЩЕЙ С ЧАСТИЦАМИ ПСЕВДООЖИЖЕННОГО СЛОЯ

Аннотация—Несмотря на то, что большинство исследователей сходятся во мнении, что теплоперенос от плотной фазы псевдоожиженного слоя является доминирующей составляющей переноса тепла от слоя к поверхности, предложенные модели процесса оказались весьма противоречивыми. Особенно заметно различие между моделями для слоев крупных частиц и при небольших временах пребывания плотной фазы. Разработана экспериментальная аппаратура, позволяющая измерять тепловое сопротивление между поверхностью и прилегающими частицами в течение быстро протекающего переходного процесса. Значимые результаты можно получить для коротких промежутков времени порядка 10 мксек. Большие значения коэффициентов теплопереноса для частиц, имеющих диаметры от 0,65 до 1,0 мм, имели место в течение первых 20 мксек. Затем, в течение следующих 80 мксек эти значения падали и почти не изменялись со временем, после чего начиналось их снижение. Такое поведение лучше всего согласуется с моделью дискретных частиц, когда начальный теплоперенос при непосредственном контакте частиц с поверхностью сменяется переносом тепла через слои газа в областях, прилегающих к точкам контакта. Существенного различия между минимально псевдоожиженными и плотными слоями с тем же числом частиц не обнаружено, что опровергает предположение о наличии слоя, отделяющего частицы от поверхности в псевдоожиженном слое.